



**HAL**  
open science

## Stagnation point heat flux characterization under numerical error and boundary conditions uncertainty

Michele Capriati, Andrea Cortesi, Thierry E Magin, Pietro M Congedo

### ► To cite this version:

Michele Capriati, Andrea Cortesi, Thierry E Magin, Pietro M Congedo. Stagnation point heat flux characterization under numerical error and boundary conditions uncertainty. *European Journal of Mechanics - B/Fluids*, 2022. hal-03707319v1

**HAL Id: hal-03707319**

**<https://inria.hal.science/hal-03707319v1>**

Submitted on 28 Jun 2022 (v1), last revised 6 Jul 2022 (v2)

**HAL** is a multi-disciplinary open access archive for the deposit and dissemination of scientific research documents, whether they are published or not. The documents may come from teaching and research institutions in France or abroad, or from public or private research centers.

L'archive ouverte pluridisciplinaire **HAL**, est destinée au dépôt et à la diffusion de documents scientifiques de niveau recherche, publiés ou non, émanant des établissements d'enseignement et de recherche français ou étrangers, des laboratoires publics ou privés.

# Stagnation point heat flux characterization under numerical error and boundary conditions uncertainty

Michele Capriati<sup>a,b,\*</sup>, Andrea Cortesi<sup>a</sup>, Thierry E. Magin<sup>b</sup>, Pietro M. Congedo<sup>a</sup>

<sup>a</sup>*Inria, Centre de Mathématiques Appliquées, Ecole Polytechnique, IPP, Route de Saclay, 91120 Palaiseau, France*

<sup>b</sup>*von Karman Institute for Fluid Dynamics, Chaussée de Waterloo 72, 1640 Rhode-Saint-Genèse, Belgium*

---

## Abstract

The numerical simulation of hypersonic atmospheric entry flows is a challenging problem. Prediction of quantities of interest, such as surface heat flux and pressure, is strongly influenced by the mesh quality using conventional second-order spatial accuracy schemes, while depending on the boundary conditions, which generally suffer from uncertainty. This paper explores these two aspects, illustrating a CFD study on the forebody of the EXPERT vehicle of the European Space Agency employing the US3D solver.

When hypersonic simulations are carried out, the mesh quality is generally assessed by checking that the difference in the quantities of interest, from a finer mesh to a coarser one, is below a fixed threshold. By contrast, in this work the numerical error on quantities of interest is systematically computed using four nested meshes. It is shown that grid adaptation tools guarantees a better trend of the numerical error and improves the order of convergence. This behavior translates into having less numerical uncertainty associated with the estimate of the quantity of interest. Secondly, boundary condition uncertainties are propagated, and a surrogate model is built for the four nested meshes for each quantity of interest. While it is common to use grid independent solutions for its building, it may be wise to compare the grid numerical uncertainty to

---

\*Corresponding author. Tel.: +39 340 96 53 013  
Email address: michele.capriati@vki.ac.be (Michele Capriati)

the one induced by the propagation study to relax this constrain. In this work, the impact of the numerical uncertainty turned out to be at least one order of magnitude less than the model variability for the chosen uncertainty space, guarantying the robustness of the surrogate model even if built on the the coarsest grid, with consequent improvement in the computational performance.

It is also shown that the importance of numerical uncertainty is reduced more by adapting the grid than by refining it. The study also pointed out how the systematic use of grid adaptation should avoid carbuncle effects that may compromise a correct heat flux estimation, with consequent impact on the surrogate model building and numerical uncertainties.

*Keywords:* atmospheric entry flows, uncertainty quantification, surrogate model, numerical error.

---

## 1. Introduction

The numerical simulation of hypersonic flows, encountered for example in atmospheric entry applications [1, 2], is a challenging problem, especially when the goal is to obtain reliable and accurate thermal loads predictions at the entry vehicle's forebody. In this context, practitioners and experts of hypersonic flows simulations know the importance of using a good computational grid to obtain accurate results. It was pointed out [3, 4, 5, 6, 7, 8] that for conventional second-order spatial accuracy schemes:

- A grid-independent solution for the pressure estimation may be inadequate for the heat flux.
- A sonic Reynolds number at the wall should be kept under the unity to compute the heat flux.
- Heat transfer prediction is not affected too much on how well resolved the shock is, but the grid must be aligned to this.
- Cells high aspect ratio in the shock region improves the estimation of the heat flux (cells stretched in shock direction).

- The choice of grid distribution depends on the numerical scheme: high dissipation schemes require higher density in the boundary layer, while low dissipation schemes need a higher quality in the shock region.
- Viscous and thermal layer are better resolved when the grid is orthogonal near the surface.

For these reasons, an excellent computational grid is a result of some grid adaptation tools and the expertise and the monitoring of an expert user [6, 9]. This expert-based strategy is normally used to produce a limited number of simulations in well-defined input conditions. The computational grid is carefully designed and adapted for the best accuracy in each case.

It is also important to note that it is not always true that a converged solution in time does imply a correct solution. It may be affected by modeling and numerical error. The first one is related to high-temperature effects (thermochemical non-equilibrium, diffusion processes, etc.), compressible effects (shock, stability, etc.), and boundary conditions (surface ablation/catalysis, etc.). The second one is related to the numerical grid used to discretize the physical domain, provided with well-suited numerical schemes. The two sources of error are coupled [10]: for example, transport proprieties rely on the computation of gradients, whose accuracy depends on the numerical grid. Such an error can be estimated by performing a rigorous grid refinement study. *Nevertheless, when hypersonic simulations are carried out, generally one is interested in obtaining a grid-independent solution. Thus, this error is normally treated in a rather pragmatic way. In fact, the analysis is commonly reduced in checking that a given quantity of interest does not notably vary between two or more differently refined mesh. By contrast, in this study, we are interested in a formal estimation of the error, which would allow to choose the most efficient numerical grid producing adequate results. Up to authors knowledge few works [11, 12] addressed specifically this topic.*

On the other hand, the modeling error can be considered by performing Uncertainty Quantification (UQ) studies. This framework must evaluate the output

quantities at several (also thousands) configurations of the uncertain input variables. Even if the associated computational cost can be alleviated by replacing the CFD model with a surrogate one, many simulations of the flow are still needed for its training. Each training simulation has to be carried out with different values of input parameters, for example, freestream values. It is clear that in this case, the user-based monitoring of the convergence of the solution is much more complex, and it can be impossible to think about doing non-automated interventions to improve the quality of the computational grid. Nonetheless, also for these applications, it is critical to have sufficiently accurate and reliable evaluations of the outputs; otherwise, fluctuations caused by numerical errors could be misinterpreted as variations due to input uncertainties or yield difficulties in the training of the surrogate model. Concerning this topic, it is essential to note that uncertainty propagation through a CFD code is often performed using a fixed mesh. In this case, a converged and well-refined mesh in nominal conditions can be reasonably regarded converged if some relatively small variations of the operating conditions are considered. This approach is usually sufficient in the absence of shock waves and non-hypersonic flows [13, 14], but it has also been used for hypersonic flows [15, 16]. In particular, in [17], a fixed computational grid, carefully adapted and refined for the nominal conditions, was used to perform all the simulations in the perturbed conditions required for the uncertainty study and the construction of a surrogate model. However, this approach can yield highly inaccurate results in hypersonic reacting flows over blunt bodies.

When considering uncertainties on some input parameters, the values of free stream conditions, such as free stream velocity or Mach number, may be subject to variations, leading to different shock stand-off distances for each sample of input parameters. This phenomenon can cause a mesh/shock misalignment and bad simulation results, provoking poor heat flux trends. When using a second-order finite-volume discretization method, a proper alignment between the shock and the discretization grid is essential to get a meaningful solution [18, 19].

This fact becomes especially challenging for UQ applications, where, to make the required simulations more affordable, one would prefer using grids that are automatically generated and not excessively refined.

We thus propose to perform a rigorous assessment of the effects of the numerical error, dependent on the mesh refinement and the uncertainties on predicting the surface pressure and heat flux on the forebody of the EXPERT vehicle [20, 21].

The two aspects are tackled separately.

First, a grid convergence study is performed on four nested meshes imposing the nominal conditions to evaluate each grid’s numerical error and uncertainty.

[The impact of employing adaptation tools on its characterization is also investigated.](#)

Anyway, when performing a UQ study, using a grid that produces relatively small uncertainty may be a waste of computational budget when the variability induced by the boundary conditions uncertainties still dominate the prediction.

For this reason, these uncertainties are propagated to estimate the variability of the quantities of interest. The latter can then be compared to the averaged numerical uncertainty to choose the best mesh employed in a UQ framework.

[The importance of using adaptation tools is also investigated when it comes to train a surrogate model.](#)

The work is structured as follows: firstly in Section 2, the CFD solver and the simulation details are given. In Section 3, the error for each used numerical domain is characterized, while in Section 4 some insights about the surrogate models and their construction are shown. The grid convergence of statistical moments is presented, together with comparing the output standard deviation and the numerical uncertainty. Finally, Section 5 draws some conclusions and perspectives.

## **2. Numerical simulations and mesh adaptation**

The results of this paper rely on the US3D software, which solves chemical reacting Navier-Stokes equations in a three-dimensional finite-volume frame-

work [22]. In this study, the numerical fluxes are computed according to the modified Steger-Warming scheme [23] with a MUSCL [24] approach to obtain second-order accuracy. The vehicle forebody flow field can be reasonably assumed to be laminar and steady. Thus, turbulence was not accounted for, neither in the modeling nor in the mesh size, and the Data Parallel Line Relaxation (DPLR [25]) time integration was employed to ensure rapid convergence to steady-state. All simulations were run until a drop of around 8 order of magnitude in the iterative residual was achieved. The high scalability and efficiency of the solver allows to reduce the computational time for each simulation, leading UQ study to be performed very cost efficiently.

The MUTATION++ library [26], already coupled to US3D in a previous work [27], is used for the closure of: I) Transport (viscosity, thermal conductivity, diffusive fluxes), II) Gas chemistry, and III) Gas-Surface interaction. Gas finite rate chemistry relies on the Park’s mechanism [28] applied to a mixture of five species air ( $S = [\text{N}, \text{O}, \text{NO}, \text{N}_2, \text{O}_2]$ ).

The surface recombination reactions, promoted by the catalytic property of the reusable Thermal Protection System (TPS) material, were accounted for; specifically,  $\text{O} + \text{O} \rightarrow \text{O}_2$  and  $\text{N} + \text{N} \rightarrow \text{N}_2$ . The surface was thus modeled imposing a surface mass-energy balance:

$$\dot{\omega}_i = \mathbf{j}_i \cdot \mathbf{n}, \quad \forall i \in S, \quad (1)$$

$$\sum_{i \in S} \mathbf{j}_i h_i \cdot \mathbf{n} - \lambda \nabla T \cdot \mathbf{n} = S_{\text{rad}}, \quad (2)$$

where  $\dot{\omega}_i$  is the chemical production term,  $\mathbf{j}_i$  the species diffusion flux,  $\mathbf{n}$  the normal to the surface,  $h_i$  the species enthalpy,  $\lambda$  the thermal conductivity and  $S_{\text{rad}} = \sigma \epsilon T^4$  the radiative energy flux (being the surface emissivity  $\epsilon = 0.9$ , and the Stefan-Boltzmann constant,  $\sigma$ ). The chemical production term was computed using a phenomenological approach, *i.e.* specifying the probability,  $\gamma$ , that a given surface reaction occurs. It reads:

$$\dot{\omega}_i = m_i \gamma_i \mathcal{N}_i, \quad (3)$$

Table 1: Nominal conditions and associated uniform uncertainties for free stream density,  $\rho_\infty$ , free stream velocity,  $u_\infty$ , and recombination probability,  $\gamma$

Variable	Nominal value	Distribution	Minimum	Maximum
$\rho_\infty$ [kg/m <sup>3</sup> ]	$2.88 \cdot 10^{-4}$	Uniform	$2.30 \cdot 10^{-4}$	$3.46 \cdot 10^{-4}$
$u_\infty$ [m/s]	4868.6	Uniform	3985.8	5842.3
$\gamma$ [-]	0.0015	Uniform	0.001	0.002

where  $\mathcal{N}_i$  is the number flux of species  $i$  impinging the wall: a probability of one indicates that all the atoms recombines at the surface, while a probability of zero implies that no reaction occurs.

The set of equations 1 and 2 is solved by means of the gas-surface interaction module of MUTATION++ [29]. It returns to the CFD solver the partial densities at the wall and its temperature,  $T_w$ . Their extrapolated values are imposed in the ghost cells as boundary condition.

In this work, we decided to simulate the entry flow of the EXPERT vehicle, using the same nominal free stream conditions as in [17], reported in table 1. In these conditions (Mach number around 15), a strong bow shock develops in front of the vehicle, as plotted in fig. 1, to adequate the streamlines to its shape. The consequent increase of temperature, fig. 2, drives the molecules dissociation into atoms. These diffuse through the boundary layer and partially recombine because of the temperature drop and the catalytic activity of the surface.

The starting nominal computational grid contains 39x41 nodes; other three finer grids were obtained by progressively doubling the nodes in both the direction to obtain geometrically similar meshes. The set of four nested grids, reported in table 2, allows to assess the spacial convergence and error of the quantities of interest. The normalized characteristic length,  $h_i/h_1$ , the wall-normal distance of the first cell at the stagnation point,  $\Delta n$ , and the average time for 5.000 iterations to be performed on 16 cores are provided in the same table.

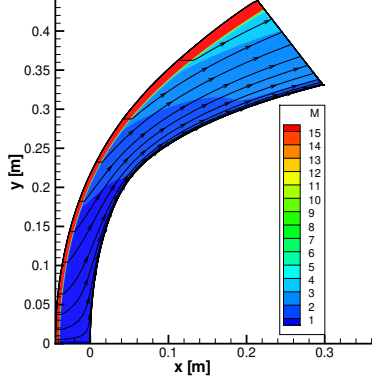


Figure 1: Mach contour at nominal condition. A strong bow shock develops in front of the vehicle to adequate the streamlines to the body shape.

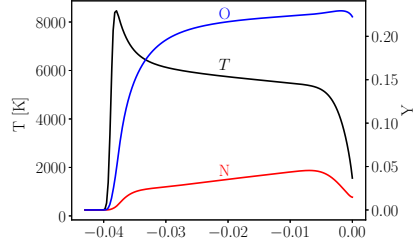


Figure 2: Temperature (left) and mass fractions (right) values along the stagnation line at nominal condition. The jump in temperature consequent to the shock drives the molecules dissociation. The resulting atoms diffuse through the boundary layer and partially recombine because of the temperature drop and the catalytic activity of the surface.

In the same table is also reported the value of the sonic Reynolds number in the stagnation point cell; it is defined as:

$$Re_c = \frac{\Delta n \rho a}{\mu_w}, \quad (4)$$

where  $\rho$  is the mixture density,  $a$  the wall sonic velocity, and  $\mu_w$  the surface viscosity, which depend on the wall state, and, thus, on the mass-energy balance imposed as boundary condition. As a general rule of thumb, hypersonic heat fluxes are well computed using a first normal spacing of  $10^{-6}$  m; anyway it was shown that this value is affected, for example, by the surface temperature [8]. A better criteria of convergence is the sonic Reynolds number, which should be kept lower than the unity [3, 4].

The mesh III and the mesh IV are showed, respectively, in fig. 3a and 3b: exploiting the axi-symmetry of the flow, the 3D problem is reduced to a 2D configuration; further reduction of the computational cost was achieved by simulating only the half part of the 2D domain.

As mentioned in the Introduction, the generation of a good mesh is a chal-

Table 2: Numerical grids used in the study: tag of the mesh, number of nodes, number of cells, normalized characteristic length,  $h_i/h_1$ , wall-normal distance of the first cell at the stagnation point,  $\Delta n$ , sonic Reynolds number based on the first physical cell, and time required to perform 5.000 iterations on 16 cores.

Mesh	Nodes	Cells	$h_i/h_1$	$\Delta n$ [m]	$Re_c$	Time [s]
I	305x321	97280	1	$1.25 \cdot 10^{-6}$	0.2	$\approx 2490$
II	153x161	24320	2	$2.50 \cdot 10^{-6}$	0.4	$\approx 675$
III	77x81	6080	4	$5.00 \cdot 10^{-6}$	0.8	$\approx 205$
IV	39x41	1520	8	$1.00 \cdot 10^{-5}$	1.6	$\approx 90$

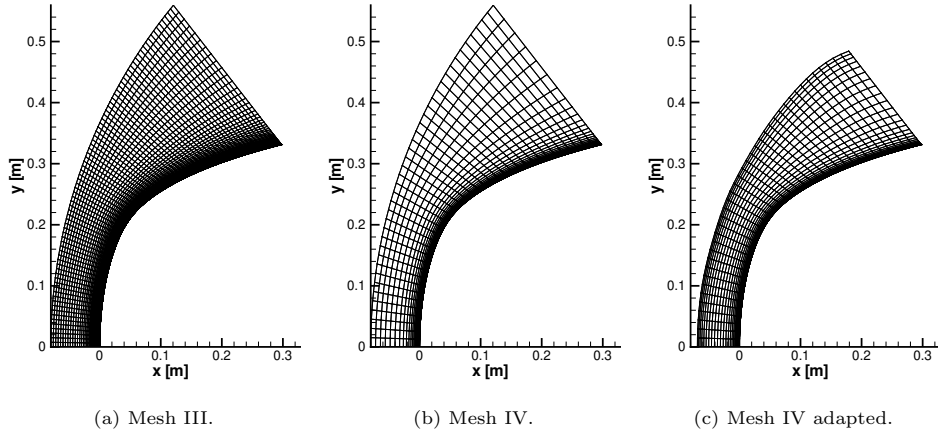


Figure 3: Numerical grids used in the study: number of nodes halved in the both the directions and effect of mesh adaptation tool.

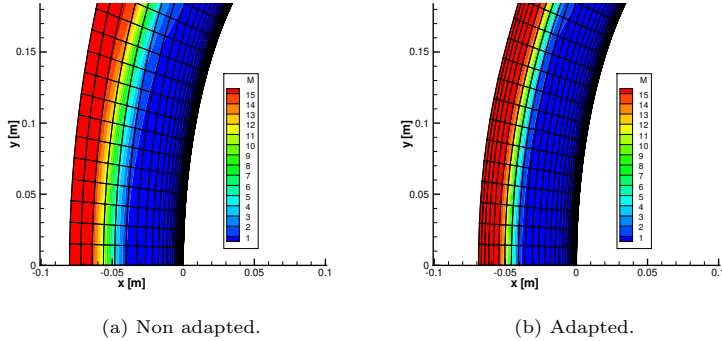


Figure 4: Zoom of the Mach contour on the mesh IV: the adaptation tool improves grid-shock alignment.

lenging task for hypersonic simulations: it is essential to align the grid to the shock [3]. This good practice reduces the magnitude of spurious numerical error produced across the shock, that, being propagated downstream, affects the correct evaluation of surface proprieties [6]. This aspect is particularly crucial in a UQ context, where building a correct mesh for each studied condition sounds as an unaffordable effort. For this reason, we used US3D “tailoring” routine [22]: once the simulation is converged on a nominal grid, the routine computes the position of the shock and the numerical grid is aligned. The simulation is then converged on the new grid. As it can be appreciate in fig. 4, the “tailoring” tool allows to capture a much less diffuse shock, improving after-shock flow predictions. An example of “tailored” is shown on fig. 3c.

### 3. Numerical error and uncertainty

When conservation laws are solved on a discretized representation of the physical domain, a numerical error,  $\epsilon_\phi$ , is inherited by the solution. This error is a function of the grid density: it approaches zero as the cell dimension approaches the infinitesimal size.

While in deterministic simulations, one is interested in estimating a grid-independent solution, *i.e.* a solution for which the discretization error is negligible, in a UQ

framework, it is possible to relax this constrain and to use a grid whose numerical uncertainty on a quantity of interest is significantly lower than the variability induced by the uncertainties.

Several methodologies for estimating such an error has been proposed in the literature. Historically, the first method was proposed by Richardson [30]: the numerical error, and, thus, the extrapolated solution, can be characterized using the solution of two nested meshes. This method assumes that the order of convergence of the numerical scheme is known and respected. To get rid of this assumption, Roache [31] proposed to use three grids for closing the system. In this study, we followed the procedure proposed by Eça [32]. Unlike the first two methods, the latter can be applied even outside the asymptotic range of spacial convergence. Considering the only highest order term, the numerical error can be approximated as:

$$\epsilon_\phi \approx \delta_{\text{RE}} = \phi_i - \phi_0 = \alpha h_i^p. \quad (5)$$

The quantity  $\phi_i$  is a flow quantity of interest at the grid refinement  $i$ ,  $\phi_0$ , the estimate of the exact solution,  $\alpha$ , a constant to be determined,  $h_i$ , the typical cell size and  $p$  is the observed order of grid convergence, that, in general, may be different from the formal one.

When the “exact” solution of the quantity of interest is not known in closed form, eq. (5) can be rearranged as follow:

$$\phi_i = \phi_0 + \alpha h_i^p. \quad (6)$$

The three unknowns ( $\phi_0$ ,  $\alpha$ , and  $p$ ) can be then estimated by using the solution of at least 4 meshes, and fitting the law [by minimizing the standard deviation,  \$\sigma\$](#) . A positive value of order of convergence ( $p$ ) guarantees a monotonic convergence, in contrast, a negative value indicates a monotonic divergence.

The method allows the numerical uncertainty associated to each mesh to be computed as:

$$U_\phi(\phi_i) = \begin{cases} F_s \epsilon_\phi(\phi_i) + \sigma + |\phi_i - \phi_{\text{fit}}|, & \text{if } \sigma < \Delta_\phi \\ 3 \frac{\sigma}{\Delta_\phi} (\epsilon_\phi(\phi_i) + \sigma + |\phi_i - \phi_{\text{fit}}|), & \text{otherwise} \end{cases}, \quad (7)$$

where  $\Delta_\phi = (\phi_i^{\max} - \phi_i^{\min}) / (n_g - 1)$  is a data range parameter which measures how distant the solutions are.  $F_s$  is a safety factor: when we have an order of convergence comparable to the theoretical one ( $0.5 \leq p < 2.1$ ) and a good quality of the fit ( $\sigma < \Delta_\phi$ ), we can safely rely on the error estimate and we prescribe a small safety factor, equal to 1.25. Contrary, the solutions lay outside the asymptotic range of convergence, and, thus, we prescribe a higher safety factor, equal to 3. Compared to other methods, such as the GCI method by Roache [31], this procedure takes into account also the uncertainty due to the scatter of data, and, being more conservative, is to be preferred in practical application, when there is not guaranty to always be in the asymptotic range. The four meshes listed in table 2 were used to compute the numerical error relative to the nominal condition reported in table 1; the results are obtained both for the adapted grids (later shown with solid lines) and for the original ones (later shown with dashed lines).

The angular distribution of pressure and heat flux are, respectively, plotted in fig. 5a and 5b; One can see the most of the numerical error concentrates around the stagnation point, where the quantities of interest reach their maximum value. Their grid dependency was investigated both as stagnation point value and as integrated value along the surface.

Equation (6) was used to compute the numerical error relative to the stagnation and integrated pressure (force), as these values fall in the monotonically convergent range. The normalized values ( $100 \cdot |\frac{\phi_i - \phi_0}{\phi_0}|$ ) are shown respectively in fig. 6a and 6c, while the corresponding orders of convergence are given on table 3. In this case, the grid adaptation tool improves the orders of convergence. These values turn out to be lower than the theoretical value of 2, expected from the MUSCL recontraction. Two main reasons compete in the corruption of the order:

- I) To prevent numerical oscillations from spreading, limiters are generally employed to decrease the order of the MUSCL extrapolation when a discontinuity, such as a shock, is detected. In this case, a mix of first and

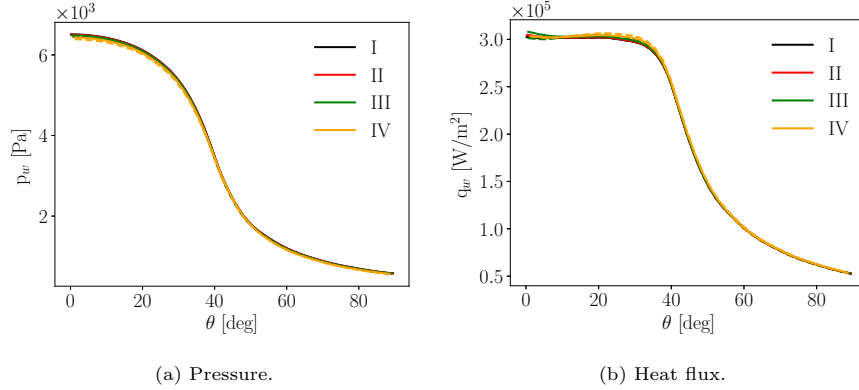


Figure 5: Angular distribution of the quantities of interest for the four meshes in table 2 relative to the nominal conditions reported in table 1. Solution from adapted mesh (A) with solid line, and from non adapted mesh (NA) in dashed line. **The numerical error concentrates around the stagnation point, where the quantities of interest reach their maximum value.**

Table 3: Orders of convergence for the quantities of interest.

	$p_w$ [Pa]	$F$ [N]	$Q$ [W]
NA	0.74	0.34	1.60
A	1.63	1.15	1.25

second-order spatial accuracy dominates the flowfield. This behaviour was already observed by Roy [12] who investigated the spatial convergence of surface pressure in a Mach 8 flow over a blunt body.

- II) The gas-surface interaction module of MUTATION++ [29], used for solving the mass-energy balance boundary condition, is first-order accurate, enforcing the first-second order mix.

Unlike these properties, stagnation point heat flux exhibits a non-monotonic convergence and equation (6) cannot be applied. In such cases, Eça [32] suggested to use a polynomial fit:

$$\phi_i = \phi_0 + \alpha_1 h_i + \alpha_2 h_i^2. \quad (8)$$

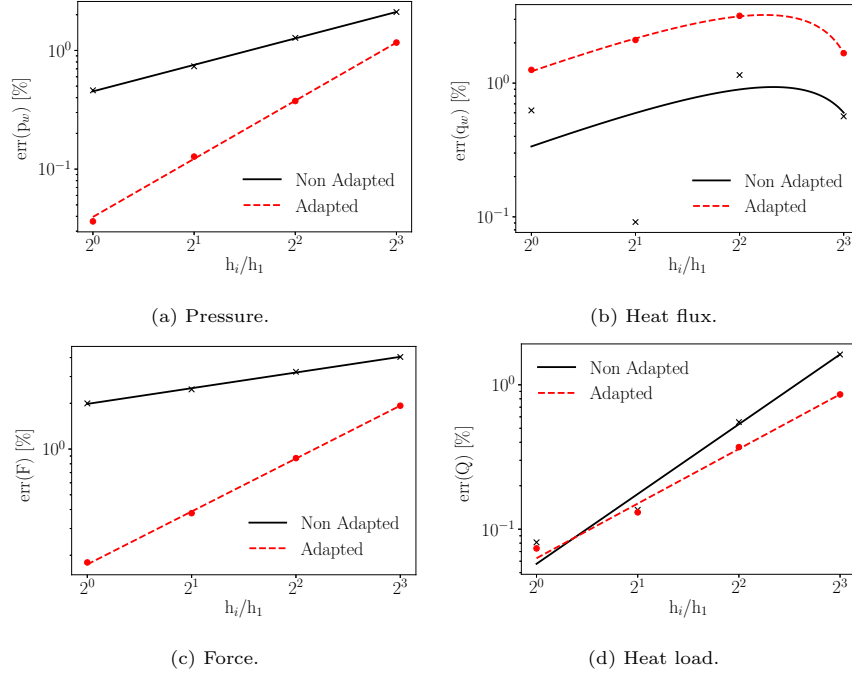


Figure 6: Relative error on the quantities of interest as function of the degree of refinement. Pressure, force and heat load in the monotonic convergence range. The observed order of convergence increases by employing grid adaption tools for pressure and force. Heat flux outside the monotonic convergence range, adaptation improves the fit.

The use of a polynomial fit is also justified by the reasons mentioned above: the error is a mix of first and second-order errors. Similarly to the other two properties, the fitting is improved when the adaptation tool is used, as one can see from fig. 6b. It is interesting to note that, by contrast, the surface integrates the value of heat flux is in the monotonic convergence range, fig. 6d.

Equation (7) allows evaluating the numerical uncertainty related to the use of a given grid, as shown in fig. 7. It can be noticed that the methodology is very conservative: the uncertainty bars of a coarser mesh contains the ones of a finer one. The only exception is the heat flux uncertainty bar of the coarsest mesh, which does not contain the other three due to the use of the polynomial fit. A second significant effect of adapting the mesh can also be noticed: the un-

certainty associated with each property decreases as a consequence of a better fitting and order of convergence.

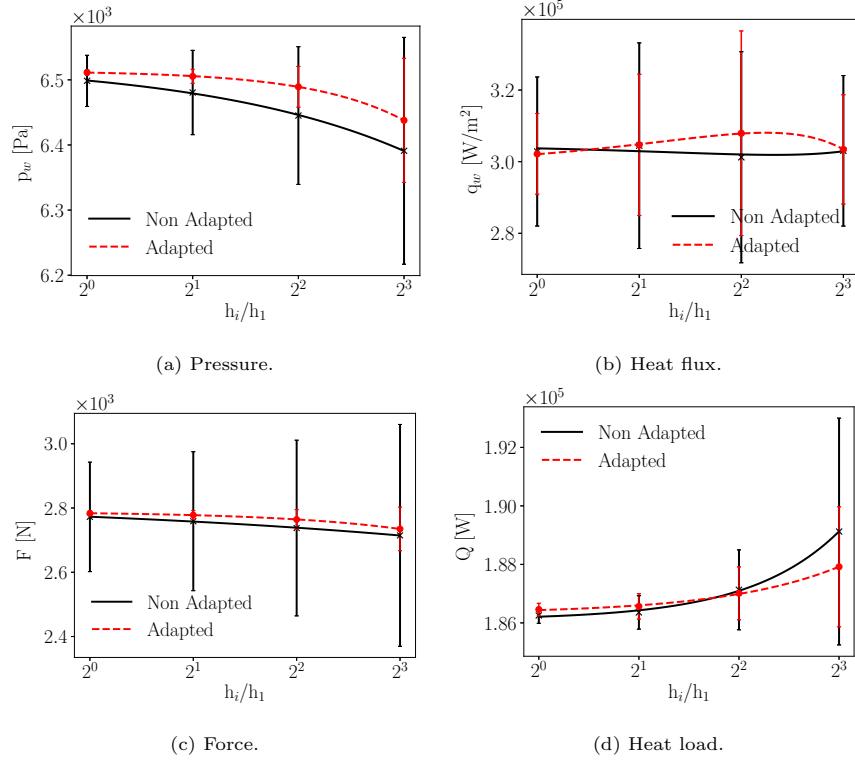


Figure 7: Quantities of interest and relative numerical uncertainty as function of the degree of refinement. The methodology is conservative: the uncertainty bars of a coarser grid consistently contain the finer grid ones; the only exception is the heat flux due to the used polynomial fit. Adaptation tools systematically reduces the numerical uncertainty.

#### 4. Uncertainty assessment and construction of a surrogate model

This section is devoted to propagating the system uncertainty through the CFD solver for a chosen computational mesh. Specifically, we estimate the confidence interval of the stagnation pressure and heat flux by propagating the

uncertain conditions on the free stream density,  $\rho_\infty$ , velocity,  $u_\infty$ , and [the re-combination probability,  \$\gamma\$](#) , of the surface of the EXPERT vehicle. For simplicity and concision, we decided to neglect the uncertainty on the atmospheric chemistry model considered in [17]. Compared to the latter work, we changed the definition of the free stream variables. Notice that this change of variables is only done for consistency with many reconstructions works in the literature. Furthermore, it does not modify the underlying problem since the free stream temperature is fixed to its nominal value and, therefore, uncertainties on the pressure are proportional to uncertainties on the density. The same can be said for Mach number and velocity since the fluid is considered a perfect gas. In this work, uninformative uniform priors are chosen for the rebuilt quantities, namely of  $\pm 20\%$  intervals around the nominal values for the density and the velocity, and a  $[0.001; 0.002]$  interval for  $\gamma$ . The complete list of uncertainties is resumed in Table 1.

In [17], Polynomial Chaos expansion was used to train surrogate models of the quantities of interest [to accelerate the Markov Chain Monte Carlo \(MCMC\) algorithm](#) used to sample the posterior distribution of the rebuilt quantities. However, due to the lack of the use of mesh adaptation, the numerical error associated with the results of heat flux simulations was too high, and the resulting surrogate model was not physically meaningful (negative heat flux values).

In this work, instead, for practical reasons, we prefer adopting an Ordinary Kriging surrogate model. The main reason is that it easily allows controlling the level of trust associated with the CFD training data, allowing for smoothing the numerical error related to heat flux simulations. Kriging interpolation is a well-known and widely-used technique for building a surrogate model; a detailed description of the model can be found in [33, 34, 35, 36]. We will not provide further details about this method in this work, but the reader can refer to the cited works for detailed descriptions. We used the UQLab software [37] for the construction of the surrogate model.

We generated  $N_s = 80$  sampling points with the Sobol technique [38] to train

the surrogate model, and  $N_v = 20$  with a Latin Hypercube strategy [39] for verification purposes.

In this study, we decided to pay the price of performing a CFD simulation for each sampling point and for the mesh I,II,III, and IV in table 2 to assess the convergence behaviour of statistical moments (mean and standard deviation). The stagnation pressure and heat flux were extracted from each solution and used to train a specific surrogate model. The surrogate model allows estimating the quantities of interest in points belonging to the uncertainty space, different from the ones used for training; the representation of the models obtained for the adapted mesh II is plotted in fig. 8. It is interesting to observe the surrogate

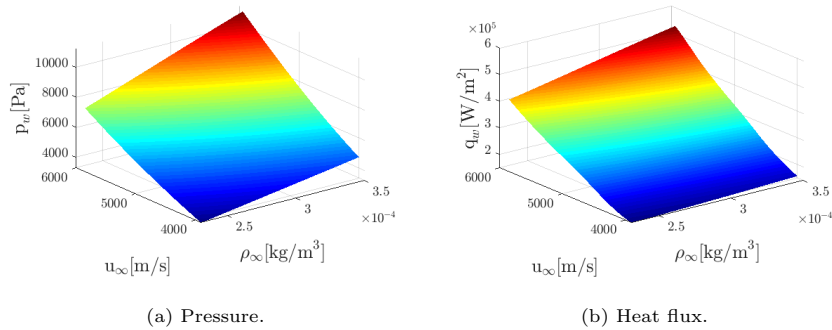


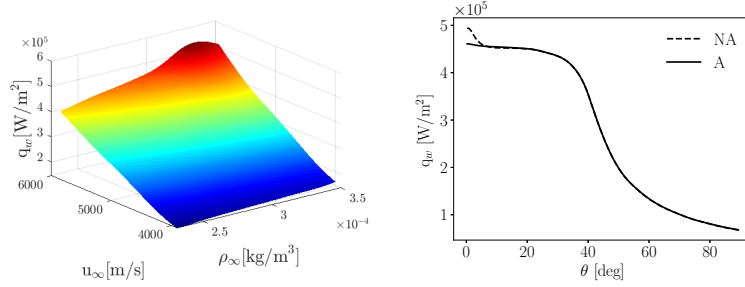
Figure 8: Surrogate models obtained for the adapted mesh II using UQLab [37]: no not physical values are observed.

built using the mesh II when the mesh is not adapted, as in fig. 9a. For the upper limit of inlet density and velocity, an overshoot in heat flux is evident: it is a consequence of the poor alignment of the grid to the shock. In particular, in fig. 9b, we can see how grid adaptation improves the solution, leading to physically sound values.

Non-physical behavior was thus not present, as instead is reported in [17], where the surrogate was predicting negative heat flux values in the portion of the range of variation of the input. We stress out that the improved quality of the surrogate model for the heat flux, with respect to [17], is not related to the different

choice of surrogate modeling technique, but it is indeed connected to the quality of the training data provided.

Furthermore, to assess the model quality, the values returned by the surrogate



(a) Surrogate model when mesh is not adapted: not physical increase in the heat flux behaviour of adapted and non adapted is predicted for high values of free stream velocity and density. (b) Angular distribution: comparison of behaviour of adapted and non adapted mesh for a free stream velocity of 5600 m/s. A not physical increase in the stagnation point region is observed when the mesh is not adapted.

Figure 9: Heat flux obtained using mesh II.

model were compared with those obtained by the CFD on the verification points. As the QQplots illustrate in fig. 10, the surrogate model performs very well, as also confirmed by the verification errors, consistently below  $10^{-5}$ . Therefore, it could be possible to safely exploit the obtained surrogates for several scopes, *e.g.* optimization, inverse problem.

Once verified the robustness of the surrogate models, they can be used to compute statistically meaningful moments, such as the mean, hereafter indicated with a  $\hat{\cdot}$  of the QoI, and the standard deviation, indicated with  $\sigma(\cdot)$  of the QoI, on the bounded uncertainty space of table 1, by means of a Monte Carlo method. As one can see in fig. 11a, the heat flux mean value of the surrogate model has the same polynomial behaviour of the heat flux in the nominal case. The same holds for the model standard deviation plotted in fig. 11b.

At this point it makes sense to compare the standard deviation of the surrogate models and the relative numerical uncertainties. We define an average

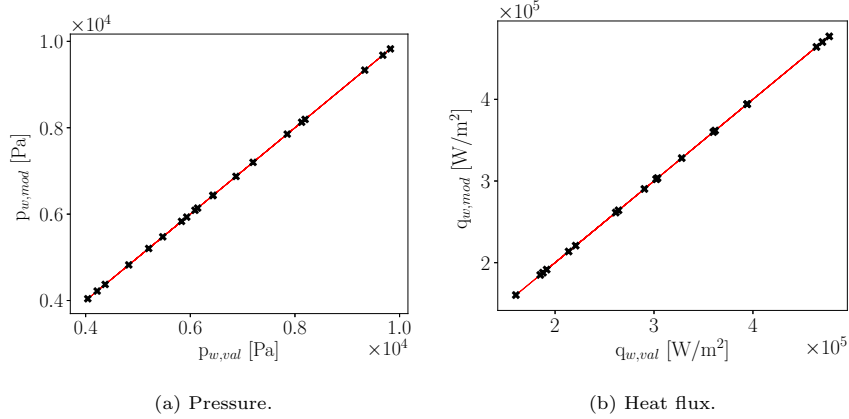


Figure 10: QQplot obtained for the adapted mesh II: the surrogate model is capable to predict correct values for the verification points.

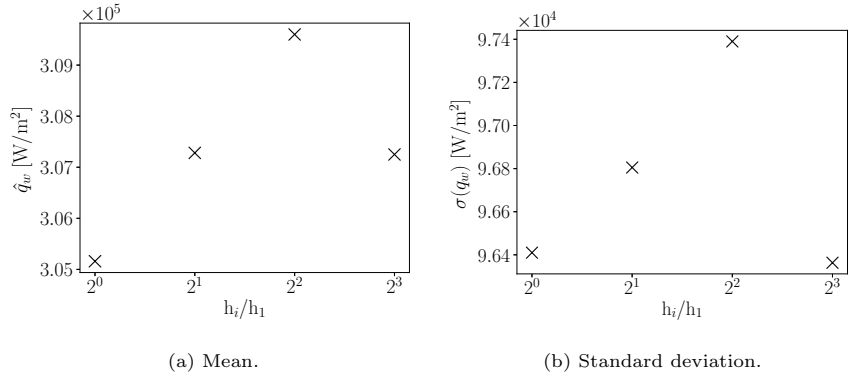


Figure 11: Statistical moments of the surrogate model relative to the uncertainty space reported on table 1, as function of the degree of refinement. They follow the same polynomial behaviour observed in the nominal case.

uncertainty, and a relative standard deviation, associated to each grid ( $g$ ) and proprieties ( $\phi$ ) as:

$$U_g(\phi) = \frac{\sum_{s=0}^{n_s} U_{g,s}(\phi)}{n_s}, \quad (9)$$

$$S_g(\phi) = \sqrt{\frac{\sum_{s=0}^{n_s} (U_g(\phi) - U_{g,s}(\phi))^2}{n_s - 1}}, \quad (10)$$

where  $U_{g,s}$  is the numerical uncertainty associated to each simulation  $s$  used to

train the surrogate model for the numerical grid  $g$ . Their values, in the case of non-adapted and adapted grids, normalized concerning the surrogate model standard deviation of each grid,  $(U_g(\phi) \pm S_g(\phi))/\sigma(\phi, h_i/h_1) \cdot 100$ , are shown in fig. 12: small ratios indicates that the numerical uncertainty is negligible compared to the one induced by the uncertainty input.

As one can see in fig. 12a, the numerical uncertainty associated with the pressure decreases with the degree of the refinement and it is systematically lower when the mesh is adapted. Moreover, it can be seen that its magnitude is reduced more by adapting the grid than by refining it. Furthermore, in the chosen uncertainty space, even the coarsest non adapted grid has a numerical uncertainty of at least one order of magnitude lower than the standard deviation, which makes the use of mesh IV for surface pressure estimate very robust.

Regarding the heat flux, in fig. 12b, the trend is not monotonic as for the pressure, but the average numerical uncertainty, and the associated standard deviation, is systematically lower in the case of the adapted grid. Remark that the significant standard deviation for the non-adapted grid is biased by few simulations where the carbuncle effect is observed. In this case, as one can see in fig. 13, the numerical uncertainty is driven high because bad scatter of the data. Adaptation, preventing the carbuncle effect from spreading, reduces the numerical uncertainty to acceptable values and is preferred in heat flux estimates.

## 5. Conclusion

In this work, we focus on building a surrogate model for representing the surface pressure and heat flux under boundary condition uncertainties.

In contrast with the common approach adopted in hypersonic simulations to assess that the quantities of interest do not sensibly vary between 2 or more differently refined meshes, we performed a systematic grid convergence study to evaluate the numerical uncertainty expected by using a given mesh. It was shown that adapting the grid reduces numerical uncertainty related to the esti-

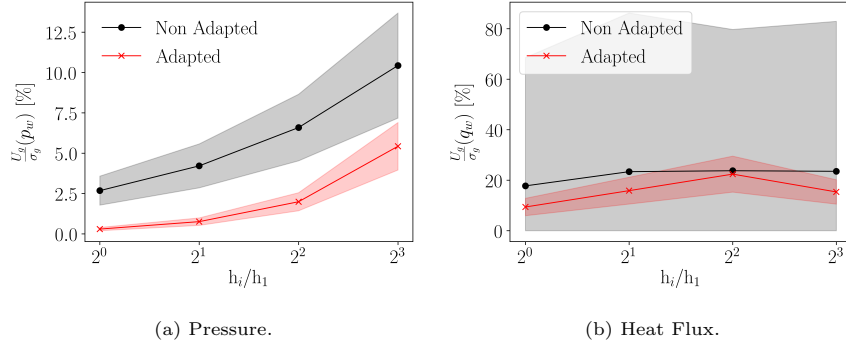


Figure 12: Ratio between the averaged grid numerical uncertainty,  $U_g(\phi)$ , and the standard deviation of the associated surrogate model,  $\sigma(\phi, h_i/h_1)$ , (solid lines), as function of the degree of refinement. Normalized standard deviation of grid numerical uncertainty,  $(S_g(\phi)/\sigma(\phi, h_i/h_1))$ , with opaque area. The numerical uncertainty is systematically lower when the mesh is adapted.

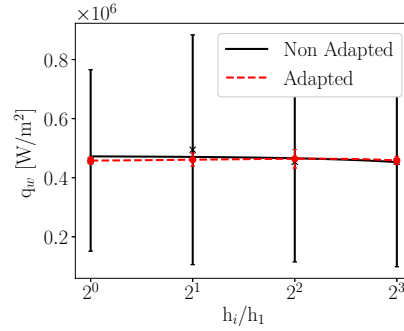


Figure 13: Numerical uncertainty as function of the degree of refinement for a free stream velocity of 5600m/s. It is driven high when carbuncle effect corrupts the solution on non adapted grids.

mate of a quantity of interest.

Secondly, a surrogate model was built for surface pressure and heat flux by propagating the system uncertainties. It was shown that adapting the grid systematically reduces numerical uncertainty; furthermore, adaptation is essential when carbuncle effects corrupt the solution and thus the convergence trend, leading to too high numerical uncertainty in the estimate. It was also pointed

out that training the surrogate models with grid independent solutions may be not the most efficient strategy. In fact, in the case study, the average numerical uncertainty turns out to be at least one order of magnitude lower than the UQ-driven standard deviation, even for the coarsest mesh. Such a numerical grid can be safely used in a UQ study: a regular behavior of the quantities of interest can be observed with a resulting good quality of the associated surrogate model. For instance, these cheap surrogates could then be used to accelerate the resolution of the inverse problem involved in the reconstruction of freestream density and velocity from stagnation pressure data.

We remind that within this work, we decide to pay the price of simulating four different meshes. From future perspectives, we will explore using adaptive methodologies to balance the numerical and the problem uncertainty to minimize the computational cost.

## 6. Acknowledgements

Authors acknowledge the Air Force Office of Scientific Research (AFOSR) for supporting the work under the grant FA9550-18-1-0209.

## References

- [1] C. Baranger, Y. Dauvois, G. Marois, J. Mathé, J. Mathiaud, L. Mieussens, A BGK model for high temperature rarefied gas flows, *European Journal of Mechanics - B/Fluids* 80 (2020) 1–12. doi:<https://doi.org/10.1016/j.euromechflu.2019.11.006>.  
URL <https://www.sciencedirect.com/science/article/pii/S0997754619303735>
- [2] Z. Bouyahiaoui, R. Haoui, A. Zidane, Numerical investigation of a hypersonic flow around a capsule in CO<sub>2</sub>-N<sub>2</sub> environment, *European Journal of Mechanics - B/Fluids* 80 (2020) 146–156. doi:<https://doi.org/10.1016/j.euromechflu.2019.12.009>.  
URL <https://www.sciencedirect.com/science/article/pii/S0997754618307775>

- [3] P. Papadopoulos, E. Venkatapathy, D. Prabhu, M. P. Loomis, D. Olynick, Current grid-generation strategies and future requirements in hypersonic vehicle design, analysis and testing, *Applied Mathematical Modelling* 23 (9) (1999) 705–735. doi:[https://doi.org/10.1016/S0307-904X\(99\)00007-4](https://doi.org/10.1016/S0307-904X(99)00007-4).  
URL <https://www.sciencedirect.com/science/article/pii/S0307904X99000074>
- [4] G. Candler, M. Barnhardt, T. Drayna, I. Nompelis, D. Peterson, P. Subbareddy, Unstructured Grid Approaches for Accurate Aeroheating Simulations. arXiv:<https://arc.aiaa.org/doi/pdf/10.2514/6.2007-3959>, doi:10.2514/6.2007-3959.  
URL <https://arc.aiaa.org/doi/abs/10.2514/6.2007-3959>
- [5] S. Henderson, J. Menart, Grid Study on Blunt Bodies with the Carbuncle Phenomenon. arXiv:<https://arc.aiaa.org/doi/pdf/10.2514/6.2007-3904>, doi:10.2514/6.2007-3904.  
URL <https://arc.aiaa.org/doi/abs/10.2514/6.2007-3904>
- [6] G. Candler, D. Mavriplis, L. Trevino, Current Status and Future Prospects for the Numerical Simulation of Hypersonic Flows. arXiv:<https://arc.aiaa.org/doi/pdf/10.2514/6.2009-153>, doi:10.2514/6.2009-153.  
URL <https://arc.aiaa.org/doi/abs/10.2514/6.2009-153>
- [7] Z.-X. Gao, H.-C. Xue, Z.-C. Zhang, H.-P. Liu, C.-H. Lee, A hybrid numerical scheme for aeroheating computation of hypersonic reentry vehicles, *International Journal of Heat and Mass Transfer* 116 (2018) 432–444. doi:<https://doi.org/10.1016/j.ijheatmasstransfer.2017.07.100>.  
URL <https://www.sciencedirect.com/science/article/pii/S0017931016324590>
- [8] S.-C. Luo, J. Liu, K. Li, Grid convergence and influence of wall temperature in the calculation of thermochemical non-equilibrium heat flux, *Journal of Physics D: Applied Physics* 53 (28) (2020) 285502. doi:10.1088/1361-

6463/ab813c.

URL <https://doi.org/10.1088/1361-6463/ab813c>

- [9] D. Saunders, S. Yoon, M. Wright, An Approach to Shock Envelope Grid Tailoring and Its Effect on Reentry Vehicle Solutions, American Institute of Aeronautics and Astronautics, 2007. arXiv:<https://arc.aiaa.org/doi/pdf/10.2514/6.2007-207>, doi:10.2514/6.2007-207.  
URL <https://arc.aiaa.org/doi/abs/10.2514/6.2007-207>
- [10] J. M. Longo, Aerothermodynamics – A critical review at DLR, Aerospace Science and Technology 7 (6) (2003) 429–438. doi:[https://doi.org/10.1016/S1270-9638\(03\)00036-1](https://doi.org/10.1016/S1270-9638(03)00036-1).  
URL <https://www.sciencedirect.com/science/article/pii/S1270963803000361>
- [11] F. G. Blottner, Accurate Navier-Stokes results for the Hypersonic Flow over a Spherical Nosedip, Journal of Spacecraft and Rockets 27 (2) (1990) 113–122. arXiv:<https://doi.org/10.2514/3.26115>, doi:10.2514/3.26115.  
URL <https://doi.org/10.2514/3.26115>
- [12] C. J. Roy, Grid Convergence Error Analysis for Mixed-Order Numerical Schemes, AIAA Journal 41 (4) (2003) 595–604. arXiv:<https://doi.org/10.2514/2.2013>, doi:10.2514/2.2013.  
URL <https://doi.org/10.2514/2.2013>
- [13] S. Kawai, K. Shimoyama, Kriging-model-based uncertainty quantification in computational fluid dynamics, American Institute of Aeronautics and Astronautics, 2014. arXiv:<https://arc.aiaa.org/doi/pdf/10.2514/6.2014-2737>, doi:10.2514/6.2014-2737.  
URL <https://arc.aiaa.org/doi/abs/10.2514/6.2014-2737>
- [14] S. Salehi, M. Raisee, M. J. Cervantes, A. Nourbakhsh, Efficient uncertainty quantification of stochastic CFD problems using sparse polynomial chaos and compressed sensing, Computers & Fluids 154 (Supplement C) (2017) 296 – 321, iCCFD8.

- [15] S. Hosder, R. Walters, R. Perez, A Non-Intrusive Polynomial Chaos Method For Uncertainty Propagation in CFD Simulations, American Institute of Aeronautics and Astronautics, 2006. arXiv:<https://arc.aiaa.org/doi/pdf/10.2514/6.2006-891>, doi:10.2514/6.2006-891.  
URL <https://arc.aiaa.org/doi/abs/10.2514/6.2006-891>
- [16] P. G. Constantine, M. Emory, J. Larsson, G. Iaccarino, Exploiting active subspaces to quantify uncertainty in the numerical simulation of the HyShot II scramjet, *Journal of Computational Physics* 302 (2015) 1–20. doi:<https://doi.org/10.1016/j.jcp.2015.09.001>.
- [17] J. Tryoen, P. M. Congedo, R. Abgrall, N. Villedieu, T. Magin, Bayesian-based method with metamodels for rebuilding freestream conditions in atmospheric entry flows, *AIAA Journal* **52** (10) (2014) 2190 – 2197.
- [18] A. Bonfiglioli, M. Grottaurea, R. Paciorri, F. Sabetta, An unstructured, three-dimensional, shock-fitting solver for hypersonic flows, *Computers & Fluids* 73 (Supplement C) (2013) 162 – 174.
- [19] M. Onofri, R. Paciorri, D. Cardillo, M. Grottaurea, A. Bonfiglioli, Numerical Simulations of flows past IXV re-entry vehicle at CRAS, in: 3rd International ARA days, 2011.  
URL <http://oldwww.unibas.it/utenti/bonfiglioli/Papersaldo/Aa-1-2011-23.pdf>
- [20] L. Walpot, H. Ottens, J.-M. Muylaert, O. Bayle, P. Urmston, U. Thomas, G. Saccoccia, M. Caporicci, C. Stavriniadis, Heat Flux and Static Stability Predictions of the Expert Vehicle, in: D. Danesy (Ed.), *Fifth European Symposium on Aerothermodynamics for Space Vehicles*, Vol. 563 of ESA Special Publication, 2005, p. 139.
- [21] A. Barrio, M. Sudars, J. Gavira, R. Aulisio, F. Ratti, F. Massobrio, L. Walpot, G. Passarelli, J. Thoemel, A. Thirkettle, EXPERT - The ESA experimental re-entry test-bed. Trajectory and mission design, 2011. doi:10.2514/6.2011-6342.

- [22] G. V. Candler, H. B. Johnson, I. Nompelis, V. M. Gidzak, P. K. Subbareddy, M. Barnhardt, Development of the US3D Code for Advanced Compressible and Reacting Flow Simulations, 53rd AIAA Aerospace Sciences Meeting (2015). arXiv:<https://arc.aiaa.org/doi/pdf/10.2514/6.2015-1893>, doi:10.2514/6.2015-1893.  
URL <https://arc.aiaa.org/doi/abs/10.2514/6.2015-1893>
- [23] J. L. Steger, R. Warming, Flux vector splitting of the inviscid gasdynamic equations with application to finite-difference methods, *Journal of Computational Physics* 40 (2) (1981) 263–293.
- [24] B. van Leer, Towards the ultimate conservative difference scheme. V. A second-order sequel to Godunov’s method, *Journal of Computational Physics* 32 (1) (1979) 101–136. doi:[https://doi.org/10.1016/0021-9991\(79\)90145-1](https://doi.org/10.1016/0021-9991(79)90145-1).  
URL <https://www.sciencedirect.com/science/article/pii/0021999179901451>
- [25] M. J. Wright, G. V. Candler, D. Bose, Data-Parallel Line Relaxation Method for the Navier-Stokes Equations, *AIAA Journal* 36 (9) (1998) 1603–1609.
- [26] J. B. Scoggins, V. Leroy, G. Bellas-Chatzigeorgis, B. Dias, T. E. Magin, Mutation++: Multicomponent Thermodynamic And Transport properties for IONized gases in C++, *SoftwareX* 12 (2020) 100575.
- [27] M. Capriati, K. Prata, T. Schwartzentruber, G. Candler, T. Magin, Development of a Nitridation Gas-Surface Boundary Condition for High-Fidelity Hypersonic Simulations, in: *WCCM-ECCOMAS2020*, 2021. doi:10.23967/wccm-eccomas.2020.119.
- [28] C. Park, R. L. Jaffe, H. Partridge, Chemical-Kinetic Parameters of Hyperbolic Earth Entry, *Journal of Thermophysics and Heat Transfer* 15 (1) (2001) 76–90.

- [29] G. Chatzigeorgis, A. Viladegut, P. Barbante, O. Chazot, T. Magin, A. Turchi, Development of catalytic and ablative gas-surface interaction models for the simulation of reacting gas mixtures, in: 23rd AIAA Computational Fluid Dynamics Conference, 2017. arXiv:<https://arc.aiaa.org/doi/pdf/10.2514/6.2017-4499>, doi:10.2514/6.2017-4499.  
URL <https://arc.aiaa.org/doi/abs/10.2514/6.2017-4499>
- [30] L. F. Richardson, R. T. Glazebrook, IX. The approximate arithmetical solution by finite differences of physical problems involving differential equations, with an application to the stresses in a masonry dam, *Philosophical Transactions of the Royal Society of London. Series A, Containing Papers of a Mathematical or Physical Character* 210 (459-470) (1911) 307–357. arXiv:<https://royalsocietypublishing.org/doi/pdf/10.1098/rsta.1911.0009>, doi:10.1098/rsta.1911.0009.  
URL <https://royalsocietypublishing.org/doi/abs/10.1098/rsta.1911.0009>
- [31] P. J. Roache, Perspective: A Method for Uniform Reporting of Grid Refinement Studies, *Journal of Fluids Engineering* 116 (3) (1994) 405–413. arXiv:<https://asmedigitalcollection.asme.org/fluidsengineering/article-pdf/116/3/405/5531128/405-1.pdf>, doi:10.1115/1.2910291.  
URL <https://doi.org/10.1115/1.2910291>
- [32] L. Eça, M. Hoekstra, A procedure for the estimation of the numerical uncertainty of CFD calculations based on grid refinement studies, *Journal of Computational Physics* 262 (2014) 104–130.
- [33] G. Matheron, The theory of regionalised variables and its applications , Ph.D. thesis, École Nationale Supérieure des Mines (1971).
- [34] N. A. C. Cressie, *Statistics for spatial data*, John Wiley & Sons, 1993.
- [35] S. N. Lophaven, H. B. Nielsen, J. Søndergaard, DACE: a MATLAB Kriging toolbox, version 2.0 , Tech. rep., Technical University of Denmark (2002).

- [36] C. E. Rasmussen, C. K. I. Williams, Gaussian processes for machine learning, The MIT Press, 2006.
- [37] S. Marelli, B. Sudret, UQLab: A Framework for Uncertainty Quantification in Matlab, pp. 2554–2563. arXiv:<https://ascelibrary.org/doi/pdf/10.1061/9780784413609.257>, doi:10.1061/9780784413609.257. URL <https://ascelibrary.org/doi/abs/10.1061/9780784413609.257>
- [38] I. Sobol', On the distribution of points in a cube and the approximate evaluation of integrals, USSR Computational Mathematics and Mathematical Physics 7 (4) (1967) 86–112. doi:[https://doi.org/10.1016/0041-5553\(67\)90144-9](https://doi.org/10.1016/0041-5553(67)90144-9). URL <https://www.sciencedirect.com/science/article/pii/0041555367901449>
- [39] M. D. McKay, R. J. Beckman, W. J. Conover, A Comparison of Three Methods for Selecting Values of Input Variables in the Analysis of Output from a Computer Code, Technometrics 21 (2) (1979) 239 – 245.

# Response to reviewers of paper EJMFLU-D-22-00038

M. Capriati, A. Cortesi, T. Magin, P. Congedo

The authors would like to thank the reviewer for his/her comments. We believe we have addressed all the issues raised by modifying the manuscript which has improved its quality.

In our response, for each comment, we have first highlighted the issue (in red), then we provided an answer, and finally we described how the manuscript was adjusted (grey box).

## Reviewer #1

### Comment #1.0

Two problems can be given: the introduction with the reference is really short, and the figure are not really discussed

We thank you for the remark. The caption of the figures were improved to fulfill with the second point. The Introduction was improved following the Reviewrs comments, as will follow.

### Comment #1.0

Another important point is the lack of originality. The original work is not specified and unclear. We can understand that several tools or library have been used, but no real development seems to have been carried out. Many conclusions are usual and can be applied to any field. One could write the same paper, just changing the flow by something else. Fluid mechanics here is not the topic. I am not sure the paper can be enough original to be publish in EJFM, and at least a strong revision is necessary.

Authors thank the Reviewer to point out the purpose of the paper was not clear. It is true that no development was carried out, at least on the numerical side. The development is mostly methodological; rather than proposing new numerical tools, the work aims at combining already existing tools and to transpose them in a field in which poor attention was previously devoted to concepts specifically targeted by this work. Even if it is true that most of the used tools may be applied to any field, authors believe fluid dynamics is still the topic. In particular for hypersonics simulations, where I) the grid dependency is mostly assessed in a pragmatic way, II) strong numerical discontinuity - shocks - may corrupt a good training of the surrogate model, as show by previous works [17]. We hope we state the research purpose in a clearer way and that the originality of the work is more evident.

#### **Comment #1.1**

Abstract is well written but original work has to be emphasized.

The authors thanks the reviewer for the advice. The two original aspects of the work have been emphasized in the abstract:

*Page 1:* When hypersonic simulations are carried out, the mesh quality is generally assessed by checking that the difference in the quantities of interest, from a finer mesh to a coarser one, is below a fixed threshold. By contrast, in this work the numerical error on quantities of interest is systematically computed using four nested meshes.

and:

*Page 1:* While it is common to use grid independent solutions for its building, it may be wise to compare the grid numerical uncertainty to the one induced by the propagation study to relax this constrain. In this work, the impact of the numerical uncertainty turned out to be at least one order of magnitude less than the model variability for the chosen uncertainty space, guarantying the robustness of the surrogate model even if built on the the coarsest grid, with

consequent improvement in the computational performance.

**Comment #1.2**

The introduction is really too much short, and does not let enough place to a real bibliography study.

We thank the Reviewer for the suggestions. A paragraph to state the gap in literature on a rigorous assessment of the numerical error in hypersonic simulations was added:

*Page 3:* Nevertheless, when hypersonic simulations are carried out, generally one is interested in obtaining a grid-independent solution. Thus, this error is normally treated in a rather pragmatic way. In fact, the analysis is commonly reduced in checking that a given quantity of interest does not notably vary between two or more differently refined mesh. By contrast, in this study, we are interested in a formal estimation of the error, which would allow to choose the most efficient numerical grid producing adequate results. Up to authors knowledge few works [11, 12] addressed specifically this topic.

A part from this specific topic, for which, up to authors knowledge, literature is pretty poor, we believe that the remaining topics are well covered in the Introduction.

**Comment #1.3**

p.3, In the introduction, the sentence “training of the surrogate model” let think that surrogate models have ever been discussed, but it is the first time. Surrogate models have to be presented before.

Thank you for pointing this out. Surrogate modeling has been introduced before:

*Page 4:* Even if the associated computational cost can be alleviated by replacing the CFD model with a surrogate one, many simulations of the flow are still needed for its training. Each training simulation has to be carried out with different values of input parameters, for example, freestream values.

**Comment #1.4**

p.3 two lines later, avoid repetition considered .. considered ..

Thanks, a synonym was used.

*Page 4:* In this case, a converged and well-refined mesh in nominal conditions can be reasonably regarded converged if some relatively small variations of the operating conditions are considered

**Comment #1.5**

end of introduction: it is not clear if the authors write an introduction or a conclusion.

Anticipations of the conclusion have been removed.

**Comment #1.6**

Section 2, beginning. The authors wrote that they have performed 3D simulations but in fact, because of the symmetry, it is a pseudo 3D, 2D axisymmetric simulation. And it explains the poor size of the mesh given in tables later (p. 6)

Yes, the consideration is correct. It is also remarked at p.7: *exploiting the axisymmetry of the flow, the 3D problem is reduced to a 2D configuration; further reduction of the computational cost was achieved by simulating only the half part of the 2D domain.*

**Comment #1.7**

Are the authors sure that the flow is steady in this configuration? We do not have any indication about the regime, laminar, transitional or turbulent. The main assumptions are not really given.

Thank you for the remark. Yes, the forebody flowfield can be values regarded laminar and steady. In each simulation the iterative residual dropped of around 8 order of magnitude. We included these assumptions in the text.

*Page 6:* The vehicle forebody flow field can be reasonably assumed to be laminar and steady. Thus, turbulence was not accounted for, neither in the modeling nor in the mesh size, and the Data Parallel Line Relaxation (DPLR [25]) time integration was employed to ensure rapid convergence to steady-state. All simulations were run until a drop of around 8 order of magnitude in the iterative residual was achieved.

**Comment #1.8**

What does it means TPS material?

We thank the Reviewer to remark that the acronym was not introduced before. It stands for Thermal Protection System, the full name has been added.

*Page 6:* The surface recombination reactions, promoted by the catalytic property of the reusable Thermal Protection System (TPS) material, were accounted for

**Comment #1.9**

In this section gamma is given as a probability, but later it is called a catalytic property (p.12). Is it the same variable with two different interpretation?

The authors thank the reviewer for pointing out this inconsistency in the nomenclature. The definition was uniformed:  $\gamma$  is the probability that an atom impinging a catalytic surface is subject to a recombination reaction.

*Page 16:* the recombination probability,  $\gamma$

Its meaning was also better clarified:

*Page 6:* It reads:

$$\dot{\omega}_i = m_i \gamma_i \mathcal{N}_i, \quad (11)$$

where  $\mathcal{N}_i$  is the number flux of species  $i$  impinging the wall: a probability of one indicates that all the atoms recombine at the surface, while a probability of zero implies that no reaction occurs.

#### **Comment #1.10**

*Page 7 :* typo: mixutre  $\rightarrow$  mixture ?

Corrected.

*Page 8:* where  $\rho$  is the mixture density

#### **Comment #1.11**

Same page: does  $\mu_w$  depend on the wall temperature? Is the wall temperature fixed, because it seems that radiation is taken into account ? please explain the boundary conditions better.

Yes, it, as well as density and wall sonic velocity, depends on the wall temperature, which is computed by means of a radiative equilibrium condition. The dependency was specified:

*Page 8:*  $a$  the wall sonic velocity, and  $\mu_w$  the surface viscosity, which depend on the wall state, and, thus, on the mass-energy balance imposed as boundary condition.

We also thank you for pointing out that the BC definition was not clear. An explanation of what is returned by the mass-energy balance, and how it is imposed in the computation, was incorporated:

*Page 7:* The set of equations 1 and 2 is solved by means of the gas-surface interaction module of MUTATION++ [29]. It returns to the CFD solver the partial densities at the wall and its temperature,  $T_w$ . Their extrapolated values are imposed in the ghost cells as boundary condition.

**Comment #1.12**

p.10, eq. 6, please explain the meaning of  $F_s$  and  $\Delta_\phi$

The description was improved as follow:

*Page 11:* by minimizing the standard deviation,  $\sigma$

*Page 12:* where  $\Delta_\phi = (\phi_1^{\max} - \phi_1^{\min}) / (n_g - 1)$  is a data range parameter which measures how distant the solutions are.  $F_s$  is a safety factor: when we have an order of convergence comparable to the theoretical one ( $0.5 \leq p < 2.1$ ) and a good quality of the fit ( $\sigma < \Delta_\phi$ ), we can safely rely on the error estimate and we prescribe a small safety factor, equal to 1.25. Contrary, the solutions lay outside the asymptotic range of convergence, and, thus, we prescribe a higher safety factor, equal to 3.

**Comment #1.13**

p.10 typo gird  $\rightarrow$  grid

Fixed.

*Page 12:* Their grid dependency was investigated both as stagnation point value and as integrated value along the surface

**Comment #1.14**

No physical phenomena are discussed from the figure. If we consider the complexity of such a flow it is really strange.

Thank you for remarking this deficit. A description of the physical phenomena has been added:

*Page 7:* In these conditions (Mach number around 15), a strong bow shock develops in front of the vehicle, as plotted in fig. 1, to adequate the streamlines to its shape. The consequent increase of temperature, fig. 2, drives the molecules dissociation into atoms. These diffuse through the boundary layer and partially recombine because of the temperature drop and the catalytic activity of the surface.

**Comment #1.15**

p.14 gamma definition unclear

We thank you for pointing out the discrepancy in gamma definition. We improved it, as answered to comment 9.

**Comment #1.16**

p. 14 What is MCMC ? (related to Monte Carlo method ?)

We thank the Reviewer to remark that the acronym was not introduced before. It stands for Markov Chain Monte Carlo, the full name was added.

*Page 16:* to accelerate the Markov Chain Monte Carlo (MCMC) algorithm

**Comment #1.17**

p.15 It will be interesting to add sampling points on the figure 6)

Yes, it would be interesting to add them. However the Fig.6 is a projection on the (u/rho) space of the surrogate model, imposing  $\gamma = \gamma_{nominal}$ . The training points lay in the (u/rho/gamma) space.

**Comment #1.18**

figure 8: for fig b, maximum of heat flux is 5 ? it is a nondimensional flux, please give indications.

The figure was badly trimmed, it is indeed the heat flux. Corrected. Thank you for the remark.

*Page 19:* QQplot obtained for the adapted mesh II: the surrogate model is capable to predict correct values for the verification points.

**Comment #1.19**

Fig 9: what is  $\hat{q}_w$  ? We can see that the order of magnitude is  $1e5$  but why the order of magnitude of sigma is so high ( $1e4$ ) ?

Thank you for pointing out the nomenclature was not specified. It was added:

*Page 18:* Once verified the robustness of the surrogate models, they can be used to compute statistically meaningful moments, such as the mean, hereafter indicated with a  $\hat{\cdot}$  of the QoI, and the standard deviation, indicated with  $\sigma(\cdot)$  of the QoI, on the bounded uncertainty space of table 1, by means of a Monte Carlo method.

It is the mean of the output space, given the uncertainties on the table 1. The standard deviation is high because the value range from less than  $1e5$  to more than  $6e5$ , see Fig. 8b

**Comment #1.20**

The discussion of fig 10 is poor.

We thank the Reviewer for the comment. The fig 10 better discussed by recalling the mathematical nomenclature in the discussion, and by explicating the purpose of the picture.

*Page 20:* Their values, in the case of non-adapted and adapted grids, normalized concerning the surrogate model standard deviation of each grid,  $(U_g(\phi) \pm S_g(\phi))/\sigma(\phi, h_i/h_1) \cdot 100$ , are shown in fig. 12: small ratios indicates that the numerical uncertainty is negligible compared to the one induced by the uncertainty input

*Page 20:* the numerical uncertainty associated with the pressure decreases with the degree of the refinement

Also the caption was improved:

*Page 21:* Ratio between the averaged grid numerical uncertainty,  $U_g(\phi)$ , and the standard deviation of the associated surrogate model,  $\sigma(\phi, h_i/h_1)$ , (solid lines), as function of the degree of refinement. Normalized standard deviation of grid numerical uncertainty,  $(S_g(\phi)/\sigma(\phi, h_i/h_1))$ , with opaque area. The numerical uncertainty is systematically lower when the mesh is adapted.

### **Comment #1.21**

Finally the conclusion does not give additional information about the originality of the work.

Thank you for the remark. Conclusion were improved:

*Page 20:* In contrast with the common approach adopted in hypersonic simulations to assess that the quantities of interest do not sensibly vary between 2 or more differently refined meshes, we performed a systematic grid convergence study to evaluate the numerical uncertainty expected by using a given mesh.

and:

*Page 21:* It was also pointed out that training the surrogate models with grid independent solutions may be not the most efficient strategy. In fact, in the case study, the average numerical uncertainty turns out to be at least one order of magnitude lower than the UQ-driven standard deviation, even for the coarsest

mesh.

**Comment #1.22**

Take care of capitals letters (for instance Navier-Stokes instead of navier-stokes)  
See refs 1, 2, 19, 20, 22, 23, 24, 27 (Ix ?), 29

Thank you to remark this. Capital letters has been corrected.

**Comment #1.23**

Some references are uncompleted, especially for AIAA publication (ref are on Arc website for AIAA conference) See refs (9, 11, 13, 17, 18 (journal?), 20,

**Comment #1.24**

Different styles are used for figures, even for simple 2D plots. That must be improved. See fig 3, 4, 5, 9, 10, 11

All fonts have been uniformed to Latex font for all the plots. Only Tecplot font was not updated, Fig. 3 and 4. Fig. 10 style was uniformed to the other 2D plots, as well as the various thickness of the lines.

**Comment #1.25**

Axis labels too much small : fig 6, 7

Font size increased. Thank you for the remark.

*Page 17:* Surrogate models obtained for the adapted mesh II using UQLab [37]:  
no not physical values are observed.

**Comment #1.26**

No x-axis label : fig 8

Fixed.

*Page 19:* QQplot obtained for the adapted mesh II: the surrogate model is capable to predict correct values for the verification points.

**Comment #1.27**

$\hat{q}$  not explained in fig 9a

Thanks to point it out. It refers to the mean of the surrogate model. The caption has been improved:

*Page 19:* Statistical moments of the surrogate model relative to the uncertainty space reported on table 1, as function of the degree of refinement. They follow the same polynomial behaviour observed in the nominal case.

**Comment #1.28**

In several figures  $h_i/h_1$  instead of  $h_i / h_1$

Fixed it.

**Comment #1.29**

Axis caption truncated (y axis, fig. 8b)

Solved.

*Page 19:* QQplot obtained for the adapted mesh II: the surrogate model is capable to predict correct values for the verification points.

**Comment #1.30**

Truncation of figures in fig 1 (along x) (0.3 is cut)

Corrected.

*Page 9:* Numerical grids used in the study: number of nodes halved in the both the directions and effect of mesh adaptation tool.